



Optimizing crash box design to meet injury criteria: a protocol for accurate simulation and material selection

Horacio Rostro-González¹ · Josep Maria Puigoriol-Forcada¹ · Armando Pérez-Peña² · Joaquin Menacho¹ · Andrés-Amador Garcia-Granada¹

Received: 3 January 2024 / Revised: 19 January 2024 / Accepted: 22 July 2024 / Published online: 28 August 2024
© The Author(s) 2024

Abstract

The design of a deformation element or crash box that meets a given injury criterion based on deceleration requires careful consideration of physical properties and space requirements. Variations in material yield stress or geometry can result in statistical variations in the injury criterion output. Optimizing the crash box to fulfil two different injury criteria and two different energy levels may require more space than initially specified. In this study, we propose a protocol where the crash box is collapsed, and force–displacement is fitted to an equation. This fit is carried out with just two simulations and compared to 30 possible scenarios, obtaining a maximum error of 38.9%. With this initial fit, the appropriate thickness and yield stress can be chosen to perform crashes with two energy levels and monitor four injury values. With the ideal yield stress and sheet metal thickness, we introduce real statistical distributions using Monte Carlo design to perform 200 simulations and obtain 400 injury values for each design proposal. This technique ensures that the design will meet injury requirements for any possible combination of thickness and yield stress accepted by quality inspection. If only one simulation is performed, all designs meet the requirements, but only the last proposed design decreased the average injury to 9.2 g with a standard deviation of 2.68 g and a maximum value of 14.4 g, which is less than the required 15 g. This technique minimizes the risk of finding combinations of yield stress and thickness that produce an undesirable injury criterion.

Keywords Crash · Monte Carlo · FEM · *HIC* · *a3ms*

1 Introduction

Crashworthiness has become an increasing research focus of the vehicle design. The main objective is to obtain a controlled deformation of the structure providing a low deceleration which minimizes injuries in car passengers or pedestrians. Warren et al. (1994) provide a review of head injury criteria (*HIC*) providing an assessment of hypothesized brain injury mechanisms, brain injury criteria, mathematical models of head injury, and available techniques for measuring head kinematics and brain tissue deformations

associated with exposure to dynamic loads. Hertz (1993) analysed candidate curves, using cadaveric data, that express the probability of skull fracture as a function of *HIC*. She concluded that a reduction in *HIC* from 1000 to 800 would result in an estimated reduction of 21.7 percent in the risk of skull fracture. With this idea of risk, many companies perform their design iterations to obtain injury values below 80% of legal requirement. This approach works as a safety factor if statistical tests lead to $80 \pm 5\%$ meaning that we meet requirements with 8 sigma.

Basic physics concepts imply that to obtain a lower deceleration we require more space to brake. If on top of that we increase initial velocity, space requirements increase dramatically. In old cars, it was possible to open the bonnet and see empty spaces that could be used for deformation but nowadays all those empty spaces are filled in with air conditioning, compressors, actuators, electronic boxes, etc. Therefore, currently the big discussion in design teams is to obtain enough deformation space in constant meeting with multidisciplinary departments. The other issue is how to

Responsible editor: Axel Schumacher

✉ Andrés-Amador Garcia-Granada
andres.garcia@iqs.url.edu

¹ GEPI-IQS Grup Enginyeria Producte Industrial, Universitat Ramon Llull, Via Augusta, 390, 08017 Barcelona, Spain

² ESI Group Hispania, S.L., Plaça Can Suris, s/n – CITILAB, Cornellà de Llobregat, 08940 Barcelona, Spain

choose the best deformation element that provides the ideal force–displacement behaviour for each required energy level.

Maine and Ashby (2002) investigated the best foam for energy absorption obtaining a very useful graph plotting in x-axis the plateau stress of each foam and in y-axis the energy per volume. They also related the minimum space requirement for pedestrian head impacts at different velocities. However, this selection was theoretical assuming that all the foam was compressed uniformly, and the acceleration was constant while compressing the foam along the stress plateau.

Zarei and Kröger (2007) performed an optimization of aluminium tubes in order to obtain the maximum energy by weight. The multi-design optimization (MDO) procedure was implemented to find an optimum filled tube that absorbed the same energy as an optimum empty tube can absorb. However, there is no link between such energy and injury values. Garcia-Granada et al. (2019) studied a topology optimization to obtain the best stiffness/weight ratio for three-point bending static loads with just one load and one objective.

Tan et al. (2021) compared foam crash box with a negative Poisson's ratio (auxetic) design. Comparing their design with traditional crash box, the peak acceleration of the car with the auxetic hierarchical crash box was reduced by 2.58%. However, real injury numbers were not provided and not even the frequency or filtering of acceleration data.

Zhou et al. (2016) used Finite Element Method with multi-objective genetic algorithm. For this optimization, they used a parametrized auxetic design of a structure. They concluded that a single indicator can be optimized successfully in the single-objective optimization. However, the other performances of the crash box may be degraded in the optimization.

All this research showed changes in acceleration curves or force displacement curves, but they did not relate to crash requirements such as $a3ms$ or head injury criteria HIC . Furthermore, they did not consider the fulfilment of different requirements in optimization.

Zeng et al. (2016) used simulations to compare to NCAP experimental crash comparing a steel beam with a composite beam. HIC was reduced by 6.37% with the new composite beam which after optimization was just 4.84% lighter than the steel part. They used a Fruit Fly Optimization Algorithm (FOA) adjusting the surface response of HIC to equation polynomial fit function of thickness of each layer of composite. For this fit, they provided minimum and maximum thickness of each layer. This optimization was possible as they were provided with more deformation space as required.

Reid and Reddy (1986) studied in 1986 the static and dynamic crushing of tapered sheet metal tubes of rectangular cross-section. They studied single-tapered and double-tapered tubes to estimate the variation of their mean

crushing forces. Mahmood and Paluszny (1981) in 1981 studied the collapse of tubes. They provided design equations and charts for sizing thin-walled structural elements for crush related to section geometry, column length, and the material properties.

Haug and Guyon (1998) linked metal forming process to obtain real thickness distributions after stamping with crash behaviour. They used an optimization loop with software from ESI® from PAM-Stamp to PAM-Crash. Ferreira et al. (2014) used FEM simulations to link the real thickness distributions from injection moulding into crash simulations.

Kim and Jeong (2010) used stochastic analysis using a MADYMO® model to calculate the sensitivity of the standard deviations of the injury numbers to the standard deviations of influential input variables to determine the most influential input variable that makes the largest contribution to the variation in the injury numbers. They managed to reduce the mean value by 9.5% and the standard deviation by 1% monitoring HIC and $a3ms$ for a frontal crash test. Brokmann et al. (2023) also used stochastic simulation to predict HIC for impacts on windshields. They provided a methodology to simulate the impact and predict the distribution of HIC values with some of them above the legal threshold. Yasuki et al. (2003) performed a similar study impacting a free motion head against interior car pillar to assure $HIC(d)$ for FMVSS201u regulation is below legal threshold. Simulations were carried out for several thickness of horizontal and vertical ribs to define the design point that would minimize the risk of going above the threshold. For all simulations, plasticity and thickness were key points to obtain a desired deformation force. Also material damping is critical for rebounds after a crash. Pérez Peña et al. (2014) provided a methodology to measure damping and compared their experimental results with ANSYS® simulations.

In this paper, we aim to achieve a crash box design that satisfies two distinct injury criteria, namely HIC and $a3ms$, for two different mass or energy levels while utilizing the smallest amount of space possible. We recognize that having more deformation space could result in weaker parts, resulting in less deceleration since there is ample space for braking.

2 Materials and methods

2.1 Compression collapse simulations for energy correlation modelling

Geometry used for a crash box might use different materials and thickness. Basic geometry is shown in Fig. 1, where a steel plate is designed with a base of $w_{xb} = 110$ mm in x direction and $w_{yb} = 120$ mm in y direction, with a stamping angle $\beta = 5^\circ$ and a total length of $L = 200$ mm which is the

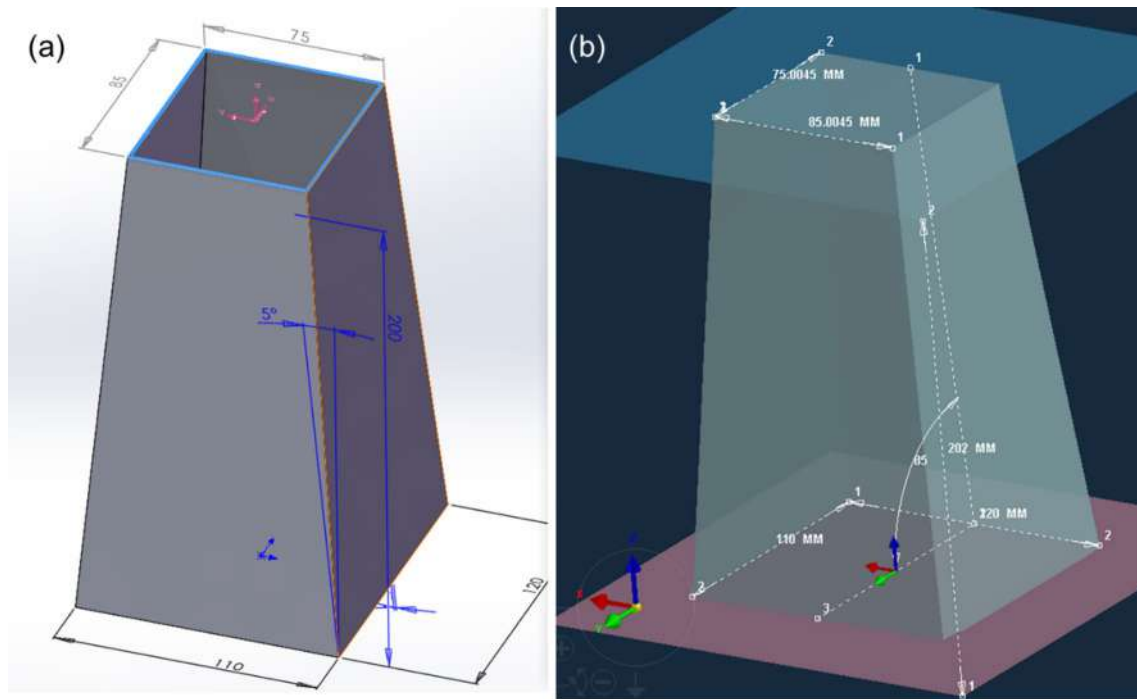


Fig. 1 Geometry of crash box from CAD (a) and in simulation (b) with top and bottom plates used for compression and impact

deformation space. The top dimensions are reduced to $w_{xt}=75$ and $w_{yt}=85$ mm, respectively, because of stamping angle $\beta=5^\circ$. The thickness of sheet metal t ranges from 0.5 to 3 mm (step 0.5 mm with standard deviation 0.1 mm). This is defined for fabrication and welding requirements. Thickness outside two times the standard deviation is rejected by quality control (this means 4.55% rejects while with six sigma or plus-minus three times standard deviation rejects would be reduced to 0.27%. With six sigma we could find plates of $1+0.3=1.3$ and plates of $1.5-0.3=1.2$ which is even smaller and for this reason we use plus-minus two sigma). With this strategy, a part with nominal thickness of 1.0 is accepted for a maximum value of 1.2 while a nominal thickness of 1.5 is accepted with a minimal value of 1.3 avoiding intersecting values. Sheet metal yield stress used in simulations range from 0.2 to 1 GPa (step 0.2 GPa) with standard deviation of 0.05GPa. Yield stress outside two times the standard deviation is rejected by quality control. With this strategy, a part with yield stress of 0.8 is accepted for a value of 0.9 and a nominal yield of 1.0 is accepted with a minimal value of 0.9 which are just touching values.

Figure 1a shows the geometry of a crash box of base 120×110 mm with angle 5° to complete a height of 200 mm. The top end decreases due to stamping angle to a rectangle 75×85 mm. The cross-section area at the top is approximately $2(75 + 82.5) \cdot t$ where t is the thickness. Figure 1b shows the implementation of CAD geometry into FEM software including top and base plates.

Coherent units (mm for length, kg for weight, and ms for time) are used in this paper for all crash simulations to express force in kN, pressure/stress in GPa, and energy in J. In Table 1, we provide coherent units used in this paper compared to some examples such as length of the thickness (0.5 to 3 mm), mass of deformation element in steel (0.3 to 1.8 kg), simulation time for energy absorption (20 ms for hard parts to 100 ms for soft parts), yield stress (0.2 to 1 GPa), and density of common materials such as plastic and steel ($1e-6$ to $8e-6$ kg/mm³). It should be noted that Young's modulus of steel is $E=200$ GPa. We also include the range of simulations for the total collapse of a deformation element.

Table 1 Coherent units

Length	Mass	Time	Force	Stress	Energy	Density ρ
mm	kg	ms	kN	GPa	$J = \text{kN} \cdot \text{mm}$	Kg/mm^3
Thickness	Defo	Simulation	F_{average}	Yield	Defo	Plastic-steel
0.5 → 3	0.5 → 1.8	20 → 100	7 → 309	0.2 → 1.0	1019 → 46,410	$1e-6 \rightarrow 8e-6$

To estimate the forces required to collapse our crash box, we divided them into categories of buckling, compression yield, elastic bending, and plastic bending. These forces are presented in Fig. 2 and compared to those obtained from a compression simulation.

For buckling, considering a straight rectangular section, we obtain high forces as follows:

$$F = \frac{\pi^2 EI}{(KL)^2} = \frac{\pi^2 200 \cdot 2 \left(\frac{75^3}{12} + \frac{85^3}{12} + 85t \left(\frac{75}{2} \right)^2 \right)}{(0.5 \cdot 200)^2} \sim 61,068 t \text{ kN}, \tag{1}$$

where E is Young’s modulus, I is the section inertia, K is the buckling factor (0.5 for fixed ends), and L is the total length. In our case, the minimum inertia is estimated around the y -axis because the width along the y -axis is greater than that along the x -axis (85 mm compared to 75 mm). For thickness values below 3 mm, the mid-term (t^3) of inertia becomes very small (less than 0.1%), allowing it to be simplified as a function of thickness. The theoretical minimum buckling force can be estimated for a minimum thickness of 0.5 mm, yielding a value of 30,534 kN, while the maximum thickness (3 mm) corresponds to a theoretical value of 183,204 kN.

To determine the yield in just compression, we assume that the compression stress is equal to the yield stress, as shown in Fig. 2. Therefore, we can derive the following equation:

$$F = \sigma_y A = \sigma_y 2(75 + 85)t = 320 \sigma_y t, \tag{2}$$

where A represents the cross-sectional area, t is the thickness, and σ_y is the yield stress. For the minimum thickness (0.5 mm) and a yield stress of 0.2 GPa, the force is estimated to be 32 kN, while for the maximum thickness (3 mm) and a maximum yield stress of 1 GPa, the force is estimated to be 960 kN. It should be noted that the average forces obtained from simulations presented in Table 1 range from 7 to 309 kN, which are slightly lower than those estimated assuming yield only in compression.

The stamping angle of $\beta = 5^\circ$ is generating a moment at each end of the crash box. Assuming that this bending stress is equal to yield stress, we obtain the following estimation of force:

$$F = \frac{\sigma_y A t}{3d} = \frac{\sigma_y 2(75 + 85)t^2}{3 \cdot 17.5} = 6.1 \sigma_y t^2 \tag{3}$$

In this case, for the minimum thickness (0.5 mm) and a yield stress of 0.2 GPa, the force is estimated to be 0.3 kN, while for the maximum thickness (3 mm) and a maximum yield stress of 1 GPa, the force is estimated to be 54 kN. It should be noted that the average forces obtained from simulations presented in Table 1 range from 7 to 309 kN, which are slightly higher than those estimated assuming elastic bending.

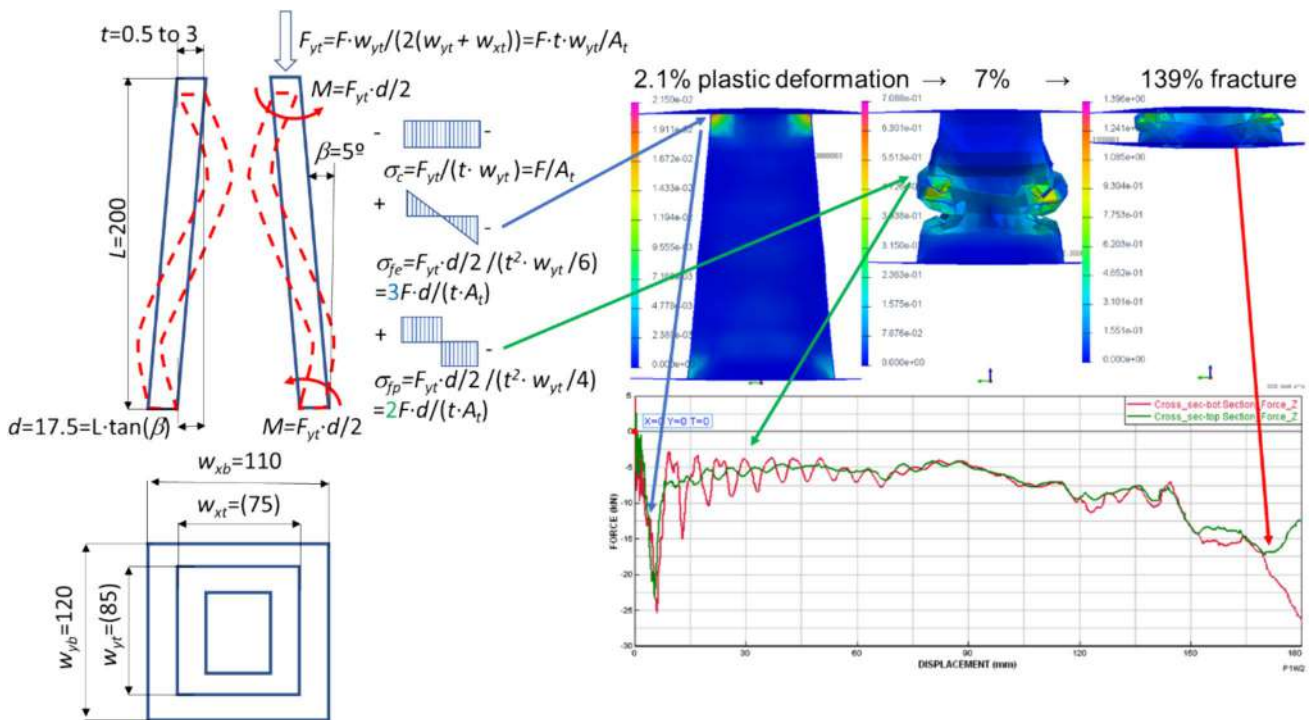


Fig. 2 Simulation of crash box collapse including equations for compression, elastic bending, and plastic bending

If the entire section experiences plastic strain during bending, the equation can be modified to account for a 50% increase in force by replacing the denominator 3 with 2. The equation becomes

$$F = \frac{\sigma_y A t}{2d} = \frac{\sigma_y 2(75 + 85)t^2}{2 \cdot 17.5} = 9.15\sigma_y t^2 \tag{4}$$

and in this case force will be in the range of 0.45 to 82 kN.

When considering both compression and bending, the force required to reach yield can be expressed as

$$F = \frac{\sigma_y A t}{(t + 3d)} = \frac{\sigma_y 2(75 + 85)t^2}{(t + 3 \cdot 17.5)} = 320\sigma_y \frac{t^2}{(t + 52.5)} \sim 6.1\sigma_y t^2 \tag{5}$$

Therefore, since compression stress is negligible compared to bending stress, the resulting expression is very similar to bending stress.

Equations 2–5 always exhibit a direct relationship between forces and yield stress, but the dependence on thickness varies: it is quadratic (power 2) for bending in Eqs. 4 and 5, linear (power 1) for compression in Eq. 3, and even includes a cubic (power 3) term for buckling in Eq. 2.

In order to obtain a model that provides a force–displacement during crash box collapse, we used finite element simulations. To perform all simulations, we designed the geometry using SolidWorks®, a 3D computer-aided design

(CAD) software, and exported it as STEP ISO 10303. This file format is a popular choice for 3D models as it is a standard for the exchange of product data.

The mesh used in the simulations was generated using 2D SHELL elements, considering the midplane surface of the geometry. An element length of 10 mm was chosen to obtain a suitable deformation shape within industrial application requirements. To simulate the bottom and top plates, we used 20 × 20 = 400 quad (4 node) elements for each plate. For the crash box, we used 1608 quad + 12 tria (3 node) elements to capture the transition from the wider base to the narrower top section (see Fig. 3).

Explicit simulations require the use of stable time step to provide accurate results. Time step for 2D elements is estimated according to the following equation:

$$t_s = fL\sqrt{\frac{\rho}{E}} = 0.00018L, \tag{6}$$

where f is a factor function of damping ratio (0.9) (Perez-Pena et al. 2014), L is the minimum element length, and ρ is the material density. For a target mesh length of 10 mm, the time step is limited to 0.0018 ms, which means that an 80-ms simulation requires 44,400 steps. A finer mesh with a 1-mm element length reduces the time step to 0.18 μs but increases the number of steps to 444,000. To ensure stability, we added a mass of 0.28 kg to the crash box (for minimum

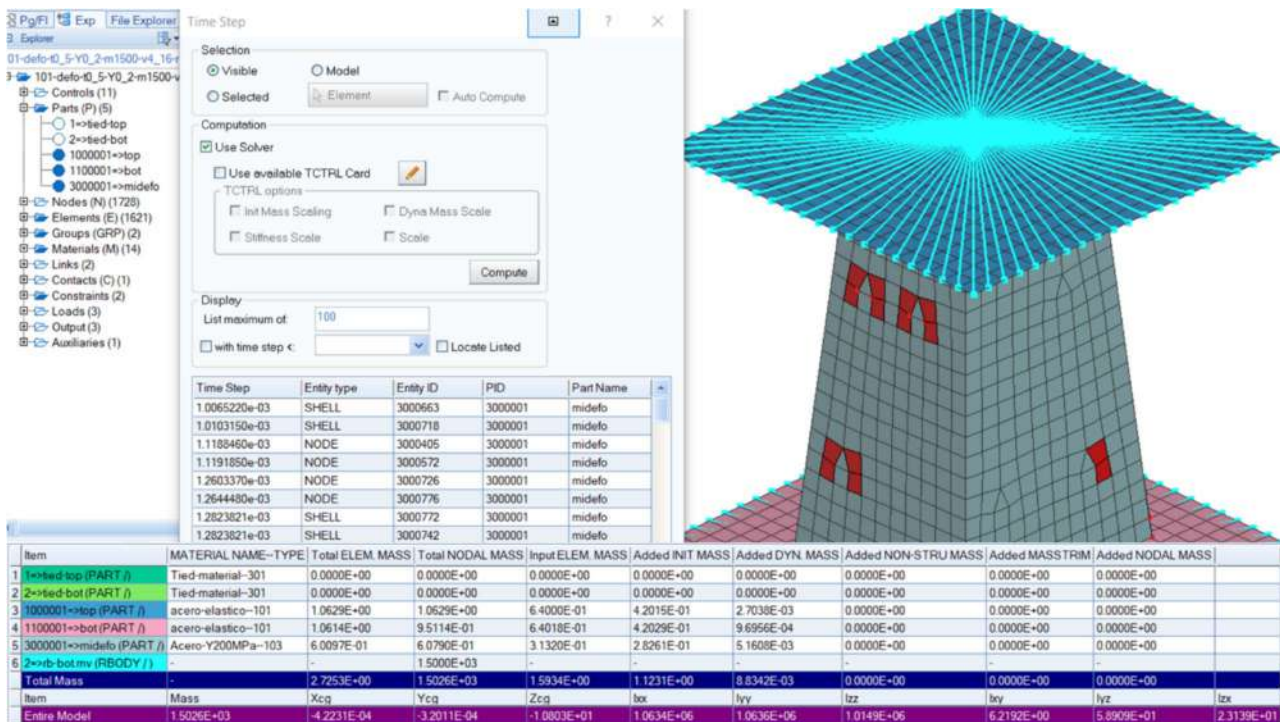


Fig. 3 Mesh details of simulation model including details of mass of each element and minimum time step elements

thickness) and set the time step to 2 μs, which is acceptable for simulations of masses over 1000 kg. However, some elements required a smaller time step of around 1 μs, which required increasing the density by a factor of 4 to obtain a time step of 2 μs. Figure 3 illustrates the small elements that required a smaller time step.

The top and bottom plates of the crash box are modelled using an elastic steel material with a thickness of 2 mm, and the edges are constrained with a rigid body. The central node of the top plate is fixed in all directions, while the central node of the bottom plate is free to move in the z direction.

Simulations 001 to 030 involve moving the bottom plate node upwards by 150 mm to compress and bend the crash box. These simulations were performed at a constant speed of 3 mm/ms, simulating 50 ms of the crash event (50 ms = 150 mm/3 mm/ms), which took 15 min to complete all 30 simulations. Simulations 101 to 130 involved a mass of 1500 kg and an initial velocity of 4.16 mm/ms (15 km/h) or an energy of 13,022 J, while simulations 201 to 230 used a mass of 1000 kg and an initial velocity of 4.16 mm/ms (15 km/h) or an energy of 8682 J. To ensure that the impact is fully resolved, a simulation time of 100 ms was used for each thickness, requiring 40 min to complete all 60 simulations.

To model the crash box, we used a range of thicknesses and yield stresses, and repeated the simulation loop for each combination. The simulation number used is shown in Table 2, where $x=0$ for compression, $x=1$ for a crash of 1500 kg or 13,022 J, and $x=2$ for a crash of 1000 kg or 8682 J. We used both yield and elastic materials to cover all possibilities, with the thickness and yield stress values changing for each iteration.

The top and bottom plates are positioned using a transformation card that can calculate for different lengths L . The plates are connected to the crash box with tie constraints to simulate a welded connection along the entire boundary.

To solve all simulations, we utilized the ESI® Virtual-Performance version 2019 software on a HP Envy Laptop with a 4-core Intel® Core™ i5-10300H CPU @2.5 GHz. The software was able to generate results for node displacement, acceleration, and section forces at 5 MHz, resulting in 20,000 points for a 100-ms simulation. We also recorded all model information, including nodal

and element data, at 1.5 kHz, which gave us 67 different time frames to work with. The output, which included image snapshots, animated gifs, and ASCII saved curves, required 32 Mb of hard disk space per simulation. This setup allowed us to automate the entire process and work with different geometries following numbering rules in separate text files: for top (1,000,000 to 1,099,999), bot (1,100,000 to 1,199,999), and defo (3,000,000 to 3,999,999). By following a consistent numbering strategy for nodes, elements, and properties, we were able to repeat the entire process without having to start from scratch, making it easier to work with new designs for deformation elements.

To obtain the average force for each combination of thickness and yield stress, the simulations 001–030 were carried out by forcing a displacement of 150 mm (prior to force increase). As shown in Fig. 2, the average force can be estimated as the energy required to crash divided by 150 mm. With this information, it is possible to fit a regression and determine the best thickness and yield stress for a given impact energy.

To minimize proportional errors, we will differentiate between total and proportional regression fit regression coefficients as follows:

Total regression fit:

The total regression fit coefficient will be calculated by fitting a linear regression model to the data of energy and the average force. This will provide an overall estimate of the relationship between energy and the average force for all combinations of thickness and yield stress. This is given by the following equation:

$$R^2_t = 1 - \frac{\sum (y_i - y_{ft})^2}{\sum (y_i - \bar{y})^2} \tag{7}$$

Proportional regression fit:

To account for the possibility of non-linear relationships between energy, thickness, and yield stress, we will also fit a proportional regression model to the data. This model will allow us to estimate the proportionality constant between energy, thickness, and yield stress for each combination of the two variables. This is given by the following equation:

Table 2 Simulation number strategy

		Thickness (mm)					
		0.5	1	1.5	2	2.5	3
Yield (GPa)	0.2	×01	×06	×11	×16	×21	×26
	0.4	×02	×07	×12	×17	×22	×27
	0.6	×03	×08	×13	×18	×23	×28
	0.8	×04	×09	×14	×19	×24	×29
	1	×05	×10	×15	×20	×25	×30

$$R^2_p = 1 - \frac{\sum \left(\frac{y_i - y_{fi}}{y_i} \right)^2}{\sum \left(\frac{y_i - \bar{y}}{y_i} \right)^2}, \tag{8}$$

where y_i is the value, y_{fi} is the fit value, and \bar{y} is the average of all values.

By using both regression models, we will be able to obtain a comprehensive understanding of the relationship between energy, thickness, and yield stress and select the best combination of variables to optimize the performance of the deformation element.

As an example, let us consider a simple set of four points with the variables x and y , as shown in Table 3. If we use the total regression formula (Eq. 7), we will obtain a 100% error for the lower value of $y = 1$, where the predicted value of y would be 0. In contrast, if we use the proportional regression formula (Eq. 8), the maximum error is only 22%, resulting in a more accurate model. Figure 4 illustrates the total regression curve y_t in red with a dashed line and the proportional y_p regression curve in green with a dash-dot line (Table 3).

Once we have obtained our best proportional fit for energy, an average force is determined, and a simple calculation for average acceleration is carried out by assuming a constant force:

$$a = \frac{F}{m}, \tag{8}$$

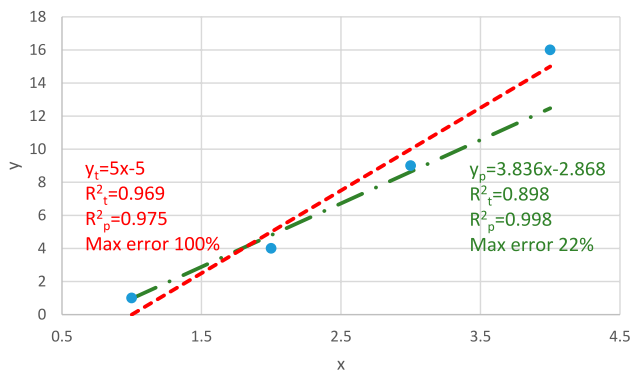


Fig. 4 Example of total versus proportional regression fit

Table 3 Regression example for total or percentage fit

x	y	y_p	$Y - y_p$	$(y - y_p)/y$	y_t	$y - y_t$	$(y - y_t)/y$
1	1	0.97	0.03	3%	0.00	1.00	100%
2	4	4.80	-0.80	-20%	5.00	-1.00	-25%
3	9	8.64	0.36	4%	10.00	-1.00	-11%
4	16	12.48	3.52	22%	15.00	1.00	6%
		R2	0.898	0.998	R2	0.969	0.975

where a is the acceleration, F is the force estimated by correlation model, and m is the mass of impact. This value can then be used to evaluate the safety of the design and make necessary adjustments.

Finally, the effectiveness of the regression in predicting injury criteria is evaluated. Two commonly used criteria, $a3ms$ and HIC (head injury criteria), are calculated based on the simulated data and compared with the results predicted by the regression. The $a3ms$ is calculated as the maximum absolute value of acceleration that lasts for 3 ms, while HIC is a measure of the likelihood of head injury, calculated based on the acceleration-time history. The HIC is calculated as

$$HIC = \max_{(t_1, t_2)} \left\{ (t_2 - t_1) \left[\frac{1}{t_2 - t_1} \int_{t_1}^{t_2} \frac{a}{g} dt \right]^{2.5} \right\}, \tag{9}$$

where a is the acceleration, g is the gravity, and t_1 and t_2 are the initial and final time of integration in seconds to obtain a maximum value. Therefore, a sustained acceleration of 100 g during 10 ms provides a value of $HIC = 1000$ s and $a3ms = 100$ g, while a sustained acceleration of 10 g during 10 ms provides a value of $HIC = 3.16$ s and $a3ms = 10$ g (For simplicity, we are considering $g = 0.01$ mm/ms² within this paper).

2.2 Simulations of impact for assuring performance

Simulations to ensure optimal performance were conducted for all combinations of thickness and yield stress, considering masses of 1000 and 1500 kg and velocity of 4.167 mm/ms (15 km/h). The primary goal was to demonstrate that the most effective method to minimize acceleration is to use the optimal design point from the compression test model. Deformation elements with low force would not be able to stop the heavy mass and would result in significant deceleration upon hitting the top plate, while elements with high force would directly produce a considerable deceleration on the moving plate.

The objective of this example is to find a deformation element that can achieve a sustained acceleration $a3ms$ below 15 g and HIC below 15 s. However, for safety reasons, the designs will target values of $a3ms < 10$ g (0.1 mm/ms²) and $HIC < 10$ s. To facilitate

the interpretation of results, a “traffic light” colour scheme will be used. Green represents values below the safety target, orange between the safety and requirement targets, and red when the targets are exceeded.

The first step before running any simulation is to determine if we have enough space to meet our safety requirements within our safety margin. To estimate the required space needed to achieve a constant deceleration, we can use the following formula:

$$z_l = \frac{v^2}{2a} = \frac{4.167^2}{2 \cdot 0.1} = 86.82 \text{ mm}, \quad (10)$$

where v is the velocity, a is the safety acceleration, and z_l is the required space for low energy.

It appears that we have adequate space to decelerate the mass with a safety acceleration. With a $L = 200$ -mm deformation element, we can utilize around 150 mm before the sheet metal plate is compressed into a hard part. However, it should be noted that if the acceleration is not constant, the required space may be doubled.

Moreover, it is crucial to estimate the time needed to stop the moving mass. Assuming a constant deceleration, the impact time can be estimated using the following formula:

$$t_{rl} = \frac{v}{a} = \frac{4.167}{0.1} = 41.67 \text{ ms}, \quad (11)$$

where v is the velocity, a is the safety acceleration, and t_{rl} is the impact required time for low-energy impact.

If we need to design the deformation element for two different impact configurations, we can obtain the required acceleration from the element with lower energy and the required space from the element with higher energy. The force required for low energy is estimated as follows:

$$F_l = m_l \cdot a = 1000 \cdot 0.1 = 100 \text{ kN}, \quad (12)$$

where F_l is the desired force for low energy, m_l is the mass for low energy, and a is the safety acceleration.

With this force, we can estimate the acceleration for the high-energy impact:

$$a_h = \frac{F_l}{m_h} = \frac{m_l}{m_h} a = \frac{1000}{1500} \cdot 0.1 = 0.066 \text{ mm/ms}^2, \quad (13)$$

where m_h is the mass for high energy and a_h is the acceleration for high energy.

Now we can estimate the space required for high energy as follows:

$$z_h = \frac{v^2}{2a_h} = \frac{v^2}{2a} \frac{m_h}{m_l} = z_l \frac{m_h}{m_l} = 86.82 \frac{1500}{1000} = 130.2 \text{ mm}, \quad (14)$$

where v is the velocity, a is the safety acceleration, and z_h is the required space for high energy. This value is already

very close to our design limitation of 150 mm for energy deformation.

In the same way, we can calculate the impact required time for high energy as follows:

$$t_{rh} = \frac{v}{a_h} = \frac{v}{a} \frac{m_h}{m_l} = t_{rl} \frac{m_h}{m_l} = 41.67 \frac{1500}{1000} = 62.5 \text{ ms} \quad (15)$$

In summary, the space required to meet two different crash requirements increases in proportion to the ratios of energy involved in each requirement. As a result, it is important to consider large simulation times for simulations that use soft deformation elements to achieve low acceleration to be sure that we can simulate the last impact with the rear wall.

3 Results and discussion

3.1 Energy absorption model of a crash box

First, we analyse the results of forced displacement for each combination of yield stress and thickness. The simulations from 001 to 030 provide a good fit to a force model that considers the following behaviour based on Eqs. 2–5:

$$F = k \cdot \sigma_y^n \cdot t^m, \quad (16)$$

where F is the force, σ_y is the yield stress, t is the thickness, and k , n , and m are parameters to fit for a good proportional regression.

In this study, we investigated the relationship between force, thickness, and yield stress for a crash box. We carried out curve fitting using different models and fitting strategies, including total and proportional fits, as well as fitting with a fixed value of $n = 1$ (from Eqs. 2–5). We also compared the results obtained from fitting with 30 simulations to those obtained using only 2 simulations for minimum (red in Table 4) and maximum (blue in Table 4) energy. The resulting models and regression coefficients are presented in Fig. 5, along with the maximum error in the estimation of energy for each model. Our findings suggest that the fitting strategy and model selection can have a significant impact on the accuracy of the energy estimation.

Table 4 shows the values of energy obtained from 30 simulations and the model fitted using just two simulations (highlighted in red and blue) with fixed value of $n = 1$, along with the corresponding values of parameter k and m . The table also displays the best option for each of the following two impact cases based on either using the 30 simulations or the fitting method.

- Case 1: For a mass of 1500 kg at 15 km/h or energy 13,022 J, both, simulation and fit, say that the best is

Table 4 Simulation of 30 cases and fit using Eq. 16 considering 30 simulations with $k=62.0737$, $n=0.830531$, $m=1.456191$

		Thickness (mm)						
		0.5	1	1.5	2	2.5	3	
Energy sim (J)								
Yield (GPa)	0.2	1019	2198	4728	6019	9790	12,090	
	0.4	1779	4512	7325	10,600	16,230	23,120	
	0.6	2476	5972	11,070	15,930	23,130	30,120	
	0.8	3574	7363	13,910	22,940	28,310	37,840	
	1	3868	8625	16,580	27,180	34,520	46,410	
Energy model (J)								
Yield (GPa)	0.2	892	2446	4415	6712	9289	12113	
	0.4	1585	4350	7851	11,936	16,519	21,542	
	0.6	2220	6092	10,994	16,715	23,133	30,167	
	0.8	2819	7736	13,962	21,226	29,376	38,308	
	1	3393	9311	16,804	25,548	35,357	46,108	
k	n	m	Diff (J)	Diff (%)	R2diff-t	R2diff-p	1-R2t	1-R2p
62.0737	0.830531	1.456191	1714	21.1%	0.996	0.999	0.0037	0.0006

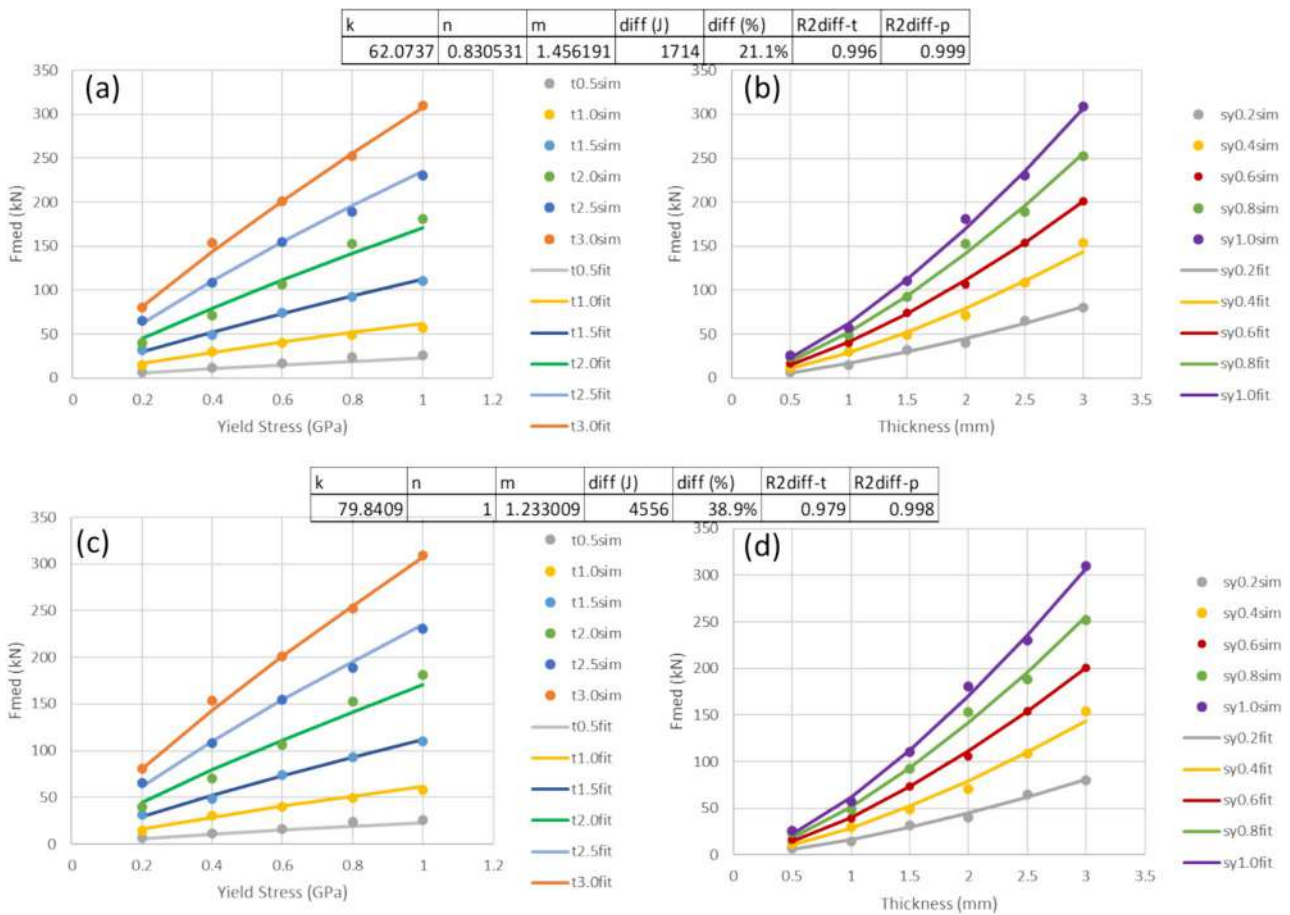


Fig. 5 Force as function of yield stress (a) and (c) and thickness (b) and (d) comparing simulation with fit results using Eq. 16. Fit results (a) and (b) obtained fitting n with 30 simulations and (c) and (d) fixing $n=1$ and just using 2 simulations for fit using minimum and maximum force

to use thickness of 1.5 mm and yield of 0.8 GPa (in green). This value of energy provides an average force of $13,022 \text{ J}/150 \text{ mm} = 86.81 \text{ kN}$ close to ideal design value of 100 kN in Eq. 12.

- Case 2: For a mass of 1000 kg at 15 km/h or energy 8682 J, both, simulation and fit, say that the best is to use thickness of 1.0 mm and yield of 1.0 GPa (in orange). This value of energy provides an average force of $8682 \text{ J}/150 \text{ mm} = 57.88 \text{ kN}$ which is significantly smaller than the design value of 100 kN in Eq. 12.

3.2 Evaluation of deceleration results using the energy absorption model

In this section, we evaluate the performance of all crash tests using the energy absorption model developed previously. We conducted 30 simulations with low energy and 30 simulations with high energy, monitoring $a3ms$ and HIC values for each simulation. This means that we monitored a total of 120 values.

In Fig. 6, we present the results of the high-energy test (1500 kg, 15 kph, 13,022 J) carried out for the minimum force (red $t = 0.5 \text{ mm}$, yield = 0.2 GPa), maximum force (blue $t = 3.0 \text{ mm}$, yield = 1.0 GPa), and designed value from force fitting (green $t = 1.5 \text{ mm}$, yield = 0.8 GPa).

In the top graph, we can see the deformation of each crash box. It is evident that the blue option is too hard, and the red option is too soft, hitting the top wall. Only the green option can absorb the energy while using most of the provided deformation space.

In the bottom graph, we monitor the acceleration versus time and the values of $a3ms$ and HIC obtained for each simulation. The hard-blue configuration provided values above the design limits for time below 22 ms, considering the elastic rebound. The soft-red configuration also provided unacceptable values for time above 50 ms when we hit the top plate. Finally, the optimized-green design shows values that are below the limits.

To evaluate the performance of different crash box designs, we have developed a comprehensive procedure based on a combination of thickness and yield stress. Figure 7 illustrates the steps involved in this procedure, which we have applied to all combinations of thickness and yield stress.

First, we subject each crash box to a compression of 150 mm, and we record the resulting energy. Then, we estimate the average force by dividing the energy by the displacement of 150 mm. Next, we estimate the average acceleration by dividing the force by the corresponding mass. Finally, we compare the predictions of this estimation of average velocity with the actual values obtained for $a3ms$ and HIC .

Our model is particularly useful for predicting the behaviour of acceleration in regions where the crash box is not too soft, i.e. where the top wall does not hit the rear wall. For our design point, which corresponds to a thickness of approximately 1.5 mm and a yield stress of 0.8 GPa, the real values of $a3ms$ and HIC are close to the predictions of constant deceleration, with errors of around 50%.

Upon analysing Fig. 7 closely, we can observe that the design point with a thickness of 1.5 mm and yield stress of 0.8 GPa is the optimal choice for a 1500-kg vehicle, in agreement with our high-energy impact prediction. Similarly, the design point with a thickness of 1.0 mm and yield stress of 1.0 GPa is the optimal choice for a 1000-kg vehicle, as predicted by our low-energy impact analysis. However, it is worth noting that there is no single design point that satisfies all four requirements of $a3ms$ and HIC for both 1000- and 1500-kg vehicles (Not all 4 values in green). To illustrate this issue, we have plotted 60 values of $a3ms$ in Fig. 8, where “h” and “l” represent the design points for high- and low-energy impacts, respectively, and we can see that only “h” design points fall outside the red area, where the regulatory requirements are not met. In Fig. 8, “h” and “l” are painted in red, orange, or green according to the value of legal requirement in this case for $a3ms$.

3.3 Multiple objective risk minimization

To ensure compliance with all 4 regulations, we conducted a comprehensive simulation study using a Monte Carlo approach to generate a normal distribution of values for thickness and yield stress. To do this, 100 values were generated, and out of these, only 2 thickness and 6 yield stress values failed to meet our quality (2 sigma) requirements. It should be noted that if we repeat this simulation many times, we expect a rejection rate of 4.55% for each parameter. We repeated the Monte Carlo simulation with 1000 values and found that 45 (4.5%) thickness values, 47 (4.7%) yield stress values, and a total of 89 (8.9%) values were out of range and thus rejected based on quality requirements. This result is in line with the expected rejection rates of 4.55% for each parameter and 8.9% for both parameters combined.

The standard deviation for thickness and yield stress is approximately 6%, but for force, it increases to 9.58% with 100 Monte Carlo points and 10.62% with 1000 points. We have a curve fit for force estimation, and Fig. 9 shows the distributions of thickness, yield stress, and estimated force for 100 and 1000 generated points.

The statistics for each Monte Carlo output of the minimum, close-to-average, and maximum thickness are provided below the figure, with red indicating values above two times the standard deviation and orange indicating values below two times the standard deviation. This table also includes the maximum and minimum possible values

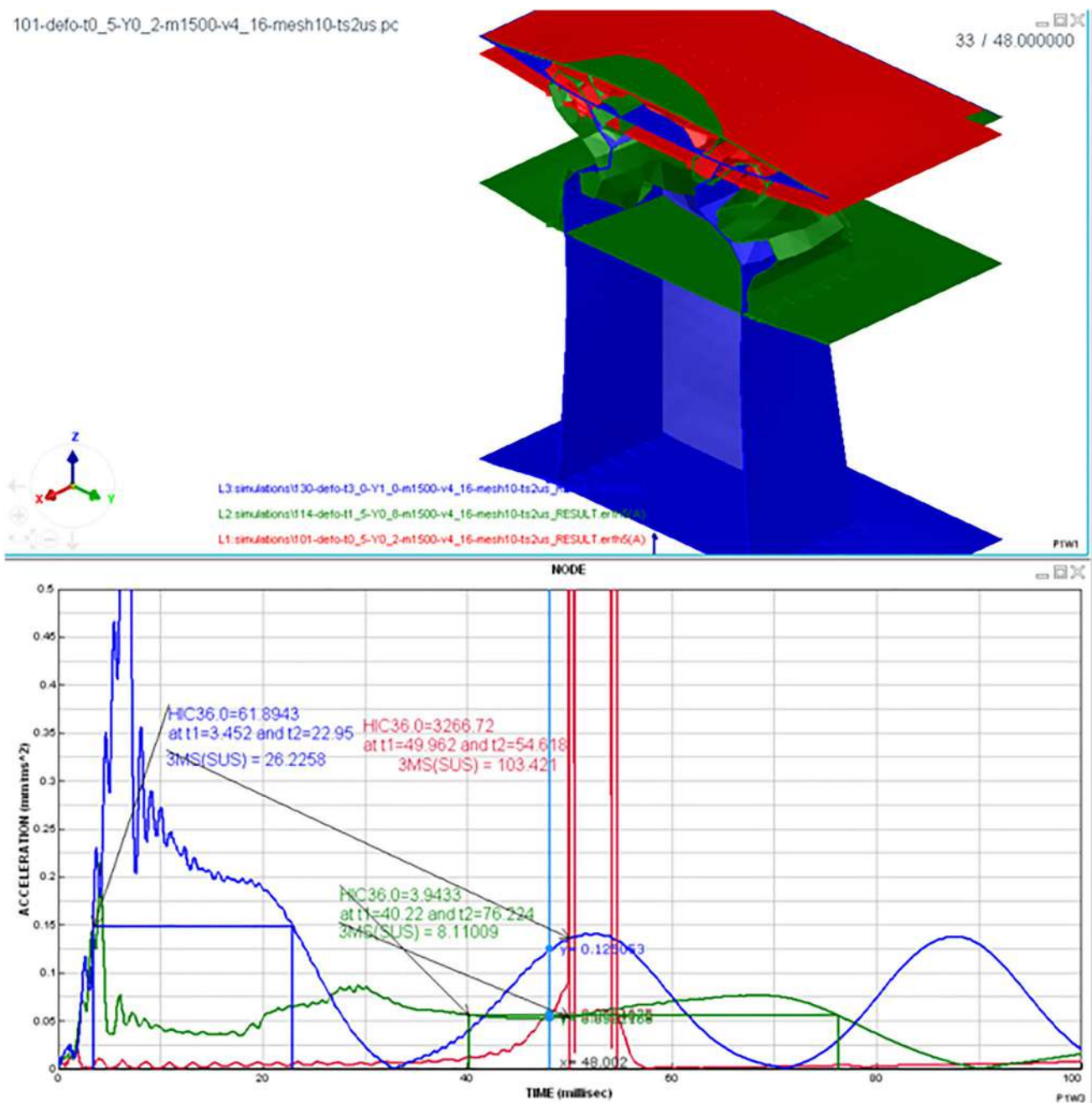


Fig. 6 Crash of 1500 kg for red = soft, green = optimum, and blue = hard deformation element

acceptable for quality. It is worth noting that if we obtain a sheet metal with the maximum allowable thickness of 1.7 mm and maximum yield stress of 0.9 GPa, we would obtain two values that do not meet the requirements. For a low-energy impact of 1000 kg, the crash box would be too hard, resulting in an $a3ms$ of 15.1 g (just above the limit) and an HIC of 21.5 s (well above the limit).

Once we generated all statistics for thickness and yield stress, we implemented a Python script to simulate 100 low-energy and 100 high-energy impacts. With this, we

aimed to assess how many injury values comply with the requirements. In total, the script generates 400 values to be checked: 100 values of $a3ms$ for low-energy impacts with 1000 kg ($a3ms-l$), 100 values of HIC for low-energy impacts with 1000 kg ($HIC-l$), 100 values of $a3ms$ for high-energy impacts with 1500 kg ($a3ms-h$), and 100 values of HIC for high-energy impacts with 1500 kg ($HIC-h$). By doing so, we can estimate the probability of meeting all four requirements simultaneously for different combinations of thickness and yield stress.



Fig. 7 Energy and force from compression used to estimate best deformation element to fulfil acceleration $a3ms$ and HIC injury criteria for 1000 and 1500 kg

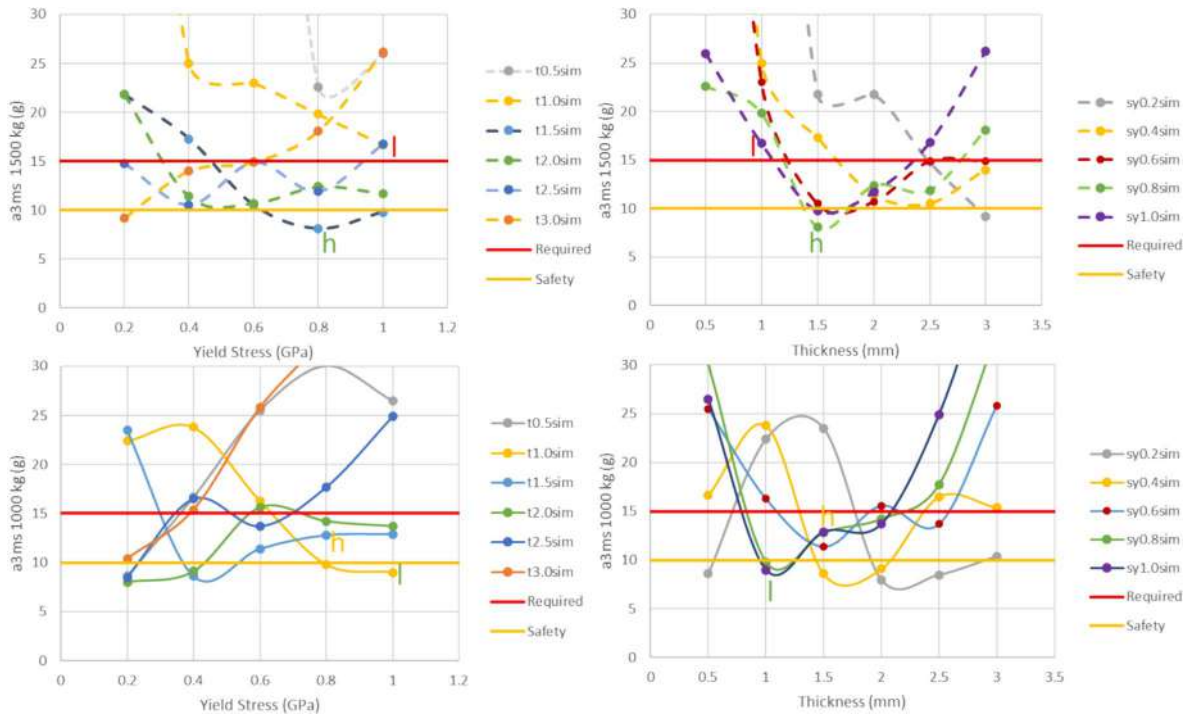


Fig. 8 Acceleration injury values $a3ms$ for crash for 1500 (top) and 1000 (bottom) kg as function of yield (left) or thickness (right)

Figure 10 shows the distribution of the 400 simulations that we generated using the Python script. It is important to note that these simulations do not follow a normal

distribution. Out of the 100 simulations for low-energy impact, 8 points (2%) did not meet the $a3ms$ requirement due to the part being too hard. Regarding the HIC for low

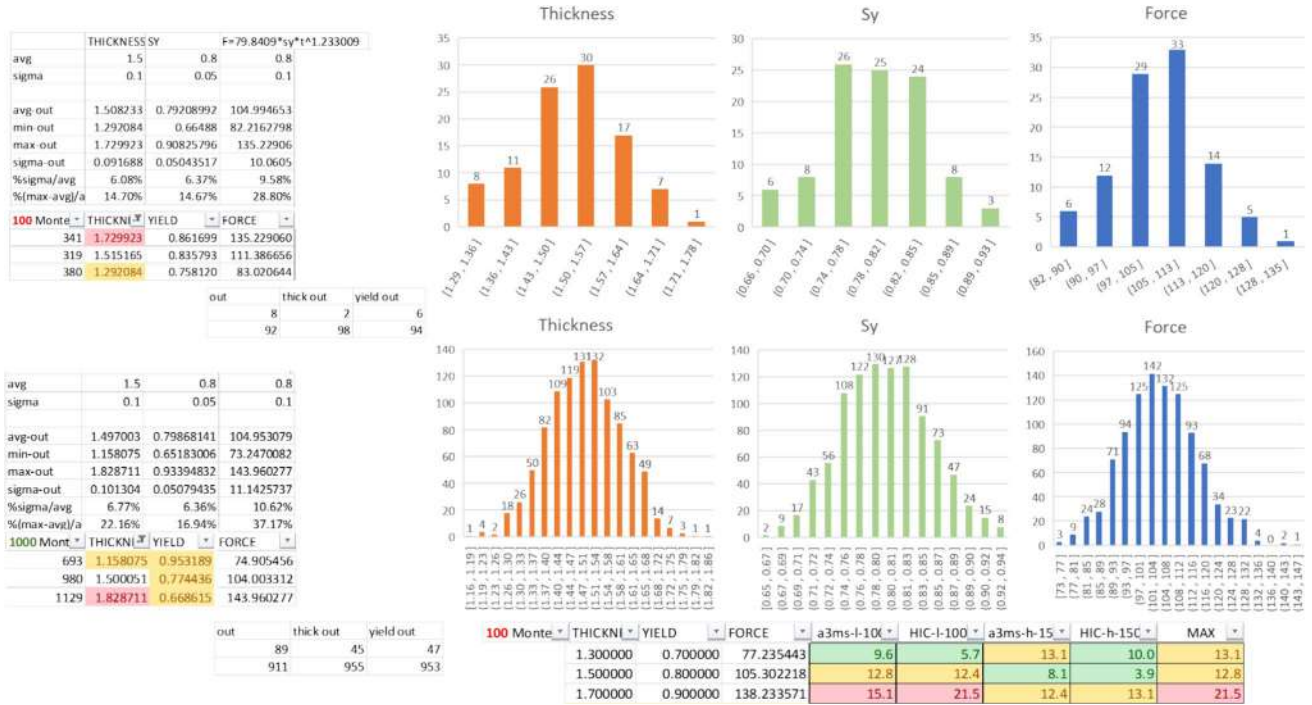


Fig. 9 Monte Carlo force estimation due to tolerances in thickness and yield stress and risk assessment

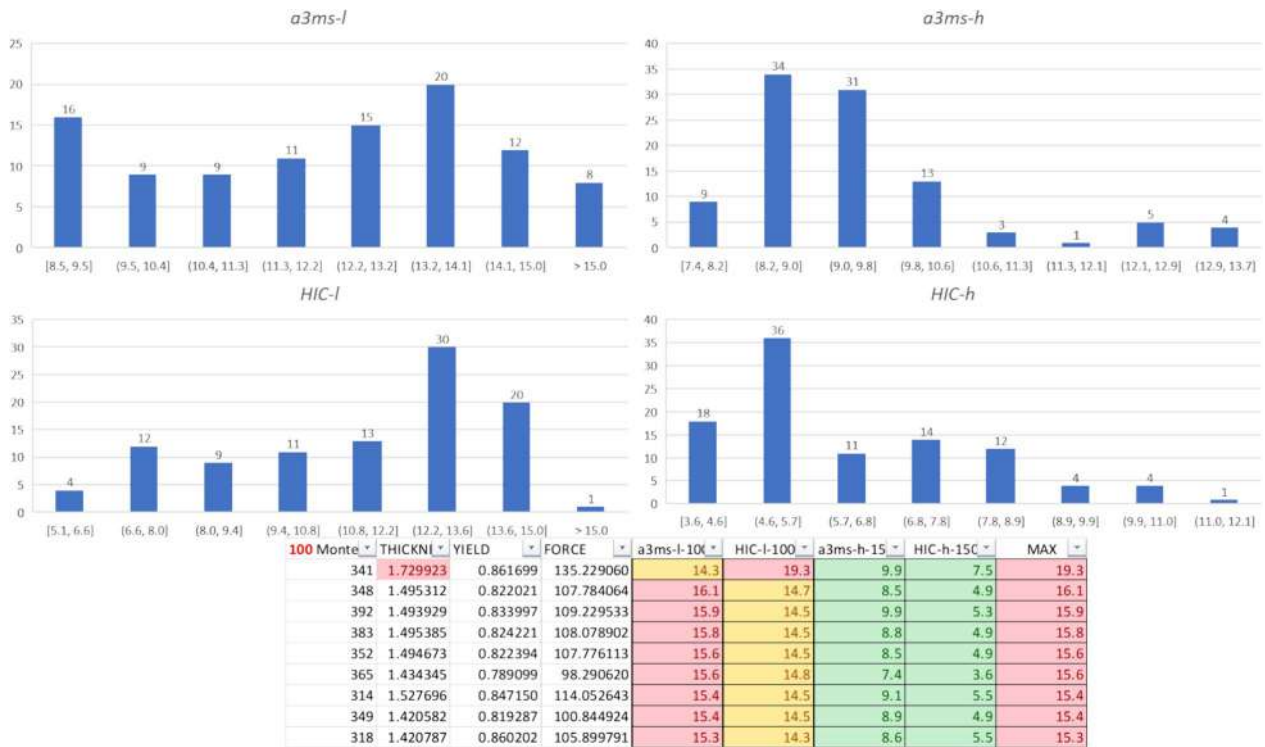


Fig. 10 Monte Carlo HIC and a3ms distribution

energy, only one point did not meet the requirement. However, this point should not be considered for production since its thickness of 1.729923 mm is above two times the standard deviation.

Figure 11 left shows the maximum value of all requirements to be met, plotted as a function of thickness and yield stress. We have divided the results into green (safety requirements), orange (just meeting the requirement), and red (above the requirement). The purple box represents the limits of yield stress and thickness that would be rejected by quality inspection. Additionally, we have plotted grey crosses representing real thickness and yield stress from parts. There is a cross relation between thickness and yield stress with an acceptable correlation factor. We have also included a black solid line to represent the probabilistic area where we find 94.54% of sheet metal thickness corresponding to ± 2 times the standard deviation.

On the right-hand side of Fig. 11, we have plotted the same 100 worst simulation values using a size bubble approach.

However, it is evident that there is still a high probability of obtaining red points within the real thickness scatter. Two extra red points are outside the probabilistic area, but they will not be rejected by quality inspection.

3.4 Design iteration for risk minimization

Simulation is a powerful tool that allows us to evaluate the risk of not meeting safety requirements. While experimental tests can be conducted to meet regulatory requirements, they do not guarantee that failure cannot occur. By utilizing simulations, we can optimize our designs by requesting 10% more space deformation and exploring different sheet metal extrusion angles. Our main goal is to find a design that meets all 400 requirements.

To simplify the process, we plot only the worst-case scenarios for each requirement (high 1500 kg vs. low 1000 kg and $a3ms$ and HIC) in Fig. 12. For each design, we perform 60 simulations to obtain 120 injury values for mapping thickness and yield stress, followed by 200 simulations for Monte Carlo scatter distribution to obtain 400 injury values. The original 200-mm design named 300 has an average injury value of 9.8, well below requirements but with 2.25% of injury values above the requirement (9 out of 400).

Model named 700 increased the length L from 200 to 220 mm and changed the extrusion angle to 3° , resulting in an average injury of 10.1 with 5.5% out of scope. Model 800 with length 220 and extrusion angle 5° obtained an average injury of 9.9 with only one value above the requirement (0.25%). We analysed this value for simulation 742 with a thickness of 1.417690488 mm and yield of 0.874338383 GPa, which resulted in HIC at low energy of 18.2, indicating that the plate was hardly deformed.

In search of a design that meets all requirements, we created new model named 900 with a 0° extrusion angle. This model showed that the nominal neighbours in the mapping met the requirements. The Monte Carlo simulation revealed that the average value decreased to 9.2 with a maximum value out of 400 of 14.4. Therefore, model 900 is the first design that meets all requirements.

Figure 12 shows the worst injury value for each iteration and the Monte Carlo outcome for the design point of thickness of 1.5 mm and yield of 0.8 GPa.

4 Conclusions

The force provided by a crash box can be modelled as a function of yield stress and thickness using the equation $F = k \cdot \sigma_y^n \cdot t^m$, where k , n , and m are parameters to be

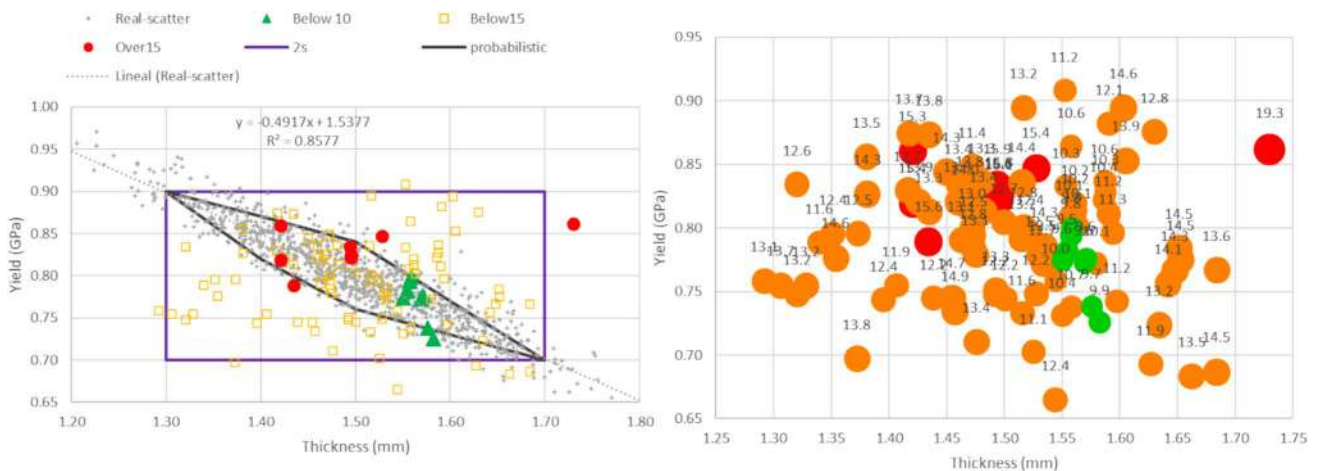


Fig. 11 Cross relation thickness versus yield stress

300		Thickness (mm)						MONTECARLO	
		0.5	1	1.5	2	2.5	3		
Yield (GPa)	0.2	6135.0	2766.0	1556.0	22.7	14.8	10.4	9.8	average
	0.4	6010.0	865.0	17.3	11.4	23.6	25.9	3.6	min
	0.6	2799.0	28.9	11.4	22.5	26.3	55.2	19.3	max
	0.8	2409.0	21.7	12.8	25.8	44.2	124.2	3.07	stddv
	1	1045.0	16.7	12.9	23.3	74.3	148.5	2.250%	cont>15

700-220-ang3		Thickness (mm)						MONTECARLO	
		0.5	1	1.5	2	2.5	3		
Yield (GPa)	0.2	6816.8	2986.0	1083.8	19.0	13.0	10.5	10.1	average
	0.4	3443.5	28.8	14.6	28.8	22.9	23.7	2.8	min
	0.6	3601.6	17.7	8.7	17.7	26.6	57.8	16.8	max
	0.8	1837.3	13.9	15.4	13.9	47.4	125.8	3.52	stddv
	1	48.2	13.1	15.9	13.1	65.1	151.6	5.500%	cont>15

800-220-ang5		Thickness (mm)						MONTECARLO	
		0.5	1	1.5	2	2.5	3		
Yield (GPa)	0.2	6500.6	2873.0	2182.8	29.9	13.5	10.2	9.9	average
	0.4	3108.5	706.1	18.4	706.1	15.6	23.7	2.8	min
	0.6	16203.1	36.5	11.4	36.5	26.2	52.8	18.3	max
	0.8	1748.6	18.9	11.0	18.9	42.9	95.6	2.28	stddv
	1	383.1	8.9	16.1	8.9	65.6	142.8	0.250%	cont>15

900-220-ang0		Thickness (mm)						MONTECARLO	
		0.5	1	1.5	2	2.5	3		
Yield (GPa)	0.2	8480.1	3380.0	40.4	17.1	10.5	11.3	9.2	average
	0.4	2956.8	38.6	12.4	38.6	14.7	26.3	2.8	min
	0.6	2536.3	17.6	11.3	17.6	23.1	58.1	14.4	max
	0.8	259.7	14.9	12.6	14.9	42.3	97.4	2.64	stddv
	1	40.1	13.4	13.1	13.4	68.8	161.2	0.000%	cont>15

Fig. 12 Iterations to minimize risk

determined. The value of n is fixed to 1 based on elastic and plastic deformation equations allowing a good fit with just two simulations. To determine the values of k and m , compression tests are carried out on the weakest and hardest possible components. The parameters are then adjusted by curve fitting, with the goal of minimizing proportional square errors between the model and simulation data. These parameters can be further estimated by an evolutionary algorithm.

The model created using 30 simulations has a maximum error of just 21.1%, indicating that it is highly accurate. However, even a simpler model created using just two simulations for the weakest and hardest configurations provides a maximum error of just 38.9% and is considered suitable for energy absorption.

When designing a crash box, it is important to consider various requirements, including $a3ms$ and HIC , while keeping space requirements in mind. Our methodology focuses on understanding the space requirements needed to achieve a safe deceleration, which is proportional to the energy ratios between different impact configurations. By carrying out low-energy simulations for a thickness of 1.0 mm and yield stress of 1.0 GPa, we obtained an optimal model that met the safety requirements for $a3ms$ and HIC , as predicted by our

curve fit of energy. Similarly, by carrying out high-energy simulations for a thickness of 1.5 mm and yield stress of 0.8 GPa, we obtained another optimal model that also met the safety requirements for $a3ms$ and HIC , as predicted by the curve fit. Through our methodology, we were able to design a crash box that fulfilled many requirements with a single configuration, allowing for safer and more efficient design.

The final crash box design, which uses a thickness of 1.5 mm and a yield stress of 0.8 GPa, was selected based on simulation results. For high-energy impact, the design meets the safety requirements for $a3ms$ and HIC , with green values. However, for low-energy impact, the design only achieves orange values for both $a3ms$ and HIC , according to deterministic simulations.

It is worth noting that the values obtained for $a3ms$ and HIC are like those predicted by the compression fitted model and constant deceleration, which assumes a constant acceleration but does not account for the time-varying acceleration curves. This highlights the importance of designing with a safety factor of 10 g (green) instead of 15 g (orange), which enables the design to meet both low- and high-energy requirements.

However, a Monte Carlo simulation with 200 samples revealed that 2% of samples may slightly exceed the 15 g

requirement for low $a3ms$ at low energy. A correlation was also found between yield stress and thickness deviations due to steel work hardening, which can affect the probability of meeting the requirements. When accounting for these deviations, the probability of non-conformance is reduced to 1.5%, but the samples would still pass quality inspection.

A final design is provided with an average worst injury value decreased to 9.2 g, a standard deviation of 2.64 g, and the most important finding that the maximum injury value is 14.4 g to guarantee that all 400 injury values are below 15 g.

Appendix

To assess the risk, we plotted the evolution of 400 injury numbers for each design, including the mean, maximum, and minimum values, as well as ± 2 times the standard deviation. As shown in Fig. 13, all models meet the legal requirements for all simulations. However, only model 900 can achieve all 400 injury numbers below the safety threshold of 15 g, which accounts for 75% of the legal requirement.

If we tabulate the 400 values and categorize them based on their values, we can create a frequency distribution that resembles a normal distribution. The design optimized at 900 shows a distribution with a much flatter curve, indicating a lower likelihood of injury values exceeding the safety threshold of 15 g.

Moreover, the frequency distribution of the injury values can also provide valuable insights into the effectiveness of the crash box design. By comparing the distributions of different designs, we can identify which

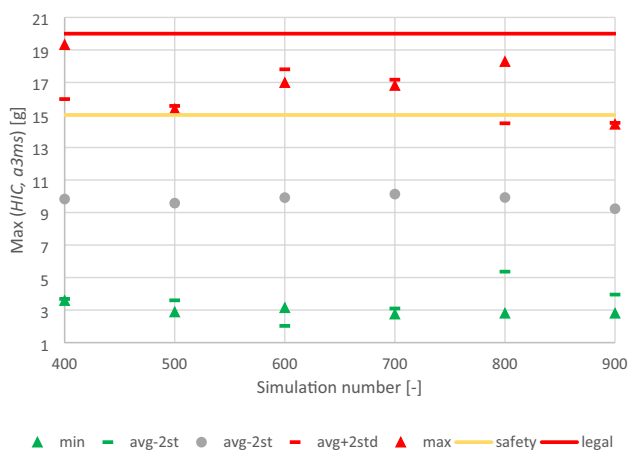


Fig. 13 Iterations to minimize risk with mean, min, max values, and standard deviations

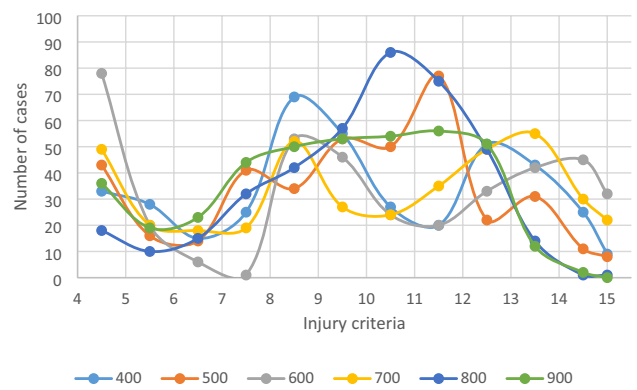


Fig. 14 Distribution of all injury numbers for each iteration showing behaviour far from normal distribution

design provides the most consistent and safe performance (Fig. 14).

Supplementary Information The online version contains supplementary material available at <https://doi.org/10.1007/s00158-024-03855-2>.

Acknowledgements This work has been performed with the support of research group GEPI which stands for Industrial Product Engineering Group (Grup Enginyeria Producte Industrial). The authors did not receive financial support from any organization for the submitted work. Thanks to this work, a grant (ACM2023_03_BioCrash) has been awarded to conduct simulations and tests of crash impacts using bioinspired designed components throughout 2024.

Author contributions A.G and H.R. wrote the main manuscript. A.P. gave support with Python scripts linked to PamCrash, J.P. completed the mesh sensitivity with time step implications for finite elements, and J.M. prepared figures with outputs from scripts. A.G. contacted automotive companies to obtain the real statistical distributions of sheet metal thickness and yield stress. All authors reviewed the manuscript.

Funding Open Access funding provided thanks to the CRUE-CSIC agreement with Springer Nature.

Data availability Data are provided within the manuscript or supplementary information files.

Declarations

Competing interests The authors have no competing interests to declare that are relevant to the content of this article.

Replication of results All simulation input decks are available for download from <https://meaagg.com/ESI/crash-methodology.zip> This compressed file includes 2 *.asc with results for a3ms and HIC injury values for all simulations; 4*.inc files with the mesh required for simulations; 261 *.pc files to be simulated with conditions for mass, velocity, thickness, and yield stress; 3 *.bat files to generate more simulations if needed; 2 *.txt with the values of yield stress and thickness used to generate the mapping and the Monte Carlo simulations; and 2*.py Python files to generate simulations and post-process such simulations.

Open Access This article is licensed under a Creative Commons Attribution 4.0 International License, which permits use, sharing, adaptation, distribution and reproduction in any medium or format, as long as you give appropriate credit to the original author(s) and the source, provide a link to the Creative Commons licence, and indicate if changes were made. The images or other third party material in this article are included in the article's Creative Commons licence, unless indicated otherwise in a credit line to the material. If material is not included in the article's Creative Commons licence and your intended use is not permitted by statutory regulation or exceeds the permitted use, you will need to obtain permission directly from the copyright holder. To view a copy of this licence, visit <http://creativecommons.org/licenses/by/4.0/>.

References

- Brokmann C, Alter C, Kolling S (2023) A methodology for stochastic simulation of head impact on windshields. *Appl Mech* 4(1):179–190. <https://doi.org/10.3390/applmech4010010>
- Ferreira V, Santos LP, Franzen M, Ghouati OO, Simoes R (2014) Improving FEM crash simulation accuracy through local thickness estimation based on CAD data. *Adv Eng Softw* 71:52–62. <https://doi.org/10.1016/j.advengsoft.2014.02.003>
- Garcia-Granada AA, Catafal-Pedragosa J, Lemu HG (2019) Topology optimization through stiffness/weight ratio analysis for a three-point bending test of additive manufactured parts. *IOP Conf Ser: Mater Sci Eng*. <https://doi.org/10.1088/1757-899X/700/1/012012>
- Hardy WN, Khalil TB, King AI (1994) Literature review of head injury biomechanics. *Int J Impact Eng* 15(4):561–586. [https://doi.org/10.1016/0734-743X\(94\)80034-7](https://doi.org/10.1016/0734-743X(94)80034-7)
- Haug E, Guyon P (1998) PAM-OPT™/PAM-SOLID™: optimization of transport vehicle crash and safety design and forming processes. <https://doi.org/10.1115/DETC98/DAC-5568>
- Hertz E (1993) A note on the head injury criterion (HIC) as a predictor of the risk of skull fracture. In: *Proceedings: association for the advancement of automotive medicine annual conference*. 37: 303–312
- Kim T-W, Jeong H-Y (2010) Stochastic analysis of the variation in injury numbers of automobile frontal crash tests. *Int J Automot Technol* 11(4):481–488. <https://doi.org/10.1007/s12239-010-0059-4>
- Mahmood HF, Paluszny A (1981) Design of thin walled columns for crash energy management—their strength and mode of collapse. *SAE Trans* 90:4039–4050
- Maine EMA, Ashby MF (2002) Applying the investment methodology for materials (IMM) to aluminium foams. *Mater Des* 23(3):307–319. [https://doi.org/10.1016/S0261-3069\(01\)00056-5](https://doi.org/10.1016/S0261-3069(01)00056-5)
- Perez-Pena A, Garcia-Granada AA, Menacho J, Molins JJ, Reyes G (2014) A methodology for damping measurement of engineering materials: application to a structure under bending and torsion loading. *J Vib Control*. <https://doi.org/10.1177/1077546314547728>
- Reid SR, Reddy TY (1986) Static and dynamic crushing of tapered sheet metal tubes of rectangular cross-section. *Int J Mech Sci* 28(9):623–637. [https://doi.org/10.1016/0020-7403\(86\)90077-9](https://doi.org/10.1016/0020-7403(86)90077-9)
- Tan H et al (2021) Crashworthiness design and multi-objective optimization of a novel auxetic hierarchical honeycomb crash box. *Struct Multidisc Optim* 64(4):2009–2024. <https://doi.org/10.1007/s00158-021-02961-9>
- Yasuki T, Okamoto A, Okamoto M (2003) Achieving design target through stochastic analysis. In: *Proceedings: international technical conference on the enhanced safety of vehicles*. Available: https://web.archive.org/web/20170210005354id_/https://www-nrd.nhtsa.dot.gov/pdf/esv/esv18/CD/Files/18ESV-000547.pdf
- Zarei HR, Kröger M (2007) Crashworthiness optimization of empty and filled aluminum crash boxes. *Int J Crashworthiness* 12(3):255–264. <https://doi.org/10.1080/13588260701441159>
- Zeng F, Xie H, Liu Q, Li F, Tan W (2016) Design and optimization of a new composite bumper beam in high-speed frontal crashes. *Struct Multidisc Optim* 53(1):115–122. <https://doi.org/10.1007/s00158-015-1312-2>
- Zhou G, Ma Z-D, Li G, Cheng A, Duan L, Zhao W (2016) Design optimization of a novel NPR crash box based on multi-objective genetic algorithm. *Struct Multidisc Optim* 54(3):673–684. <https://doi.org/10.1007/s00158-016-1452-z>

Publisher's Note Springer Nature remains neutral with regard to jurisdictional claims in published maps and institutional affiliations.